

# Strength reduction of mudstone embankment due to change in water content

Tetsuo Abe<sup>(1)</sup>, Yuki Hashimoto<sup>(2)</sup>, Nobuo Mishima<sup>(3)</sup>, Shima Kawamura<sup>(4)</sup>

## Abstract

In August 2009, the Suruga Bay earthquake caused the collapse of an embankment on the Tomei Expressway, Japan. According to later investigation, the main cause was the embankment materials with slaking property became finer due to the seepage of rainwater and groundwater, and the embankment caused a decrease in strength. However, since it has been known that the fine granulation of the embankment materials by slaking will be completed in about 10 years after the construction, in actual, the collapsed embankment has been in service for 40 years. The authors do not evaluate that the fine granulation is the only cause of the collapsed embankment. Instead, we focused on the fact that the water content increased with the granulation, and confirmed the effect of the increase in water content on strength behavior by experiments. The results indicated that the reduction in strength of embankments made of slaking materials depends not only on the fine granulation of the embankment materials, but also on the increase in water content.

**Key words:** mudstone, embankment, slaking, fine granulation, water content, strength reduction

## 1. Introduction

In August 2009, a magnitude 6.5 earthquake that occurred in Suruga Bay off the coast of Omaezaki, Shizuoka Prefecture, Japan, caused a disaster that resulted in the collapse of the embankment of the Tomei Expressway. Later investigation, clarified that the main cause was the embankment materials with slaking property. Neogene mudstone, became gradually finer and finer over time due to repeated dry and wet conditions caused by seepage of rainwater and groundwater, this process resulted in a decrease in the strength of the embankment (Takagi et al., 2010). However, it has been generally said that the fine granulation of embankment materials by slaking is completed about 10 years after the embankment construction (Nakamura, 2014). Since the embankment that collapsed was already in service 40 years ago, therefore, we evaluated that the fine granulation of the embankment materials was not the only cause of the embankment collapse. In this study, we focused on the fact that the water content of embankment materials made of slaking materials such as mudstone increases as the materials become finer due to slaking, and confirmed the effect of the increase in water content on strength behavior by experiments.

## 2. Experiments

### 2.1. Soil materials used in the experiments

The physical properties of the soil used in the experiments are shown in Table 1. This soil material (referred to as "Kobe 5") was sampled from the ground near the Kobe Junction during the construction of the Shin-Meishin Expressway between Takatsuki and Kobe, which was in service in March 2018, and is mainly mudstone with slaking property. The stratum containing this mudstone has been called the "Kobe Group", which was formed 32-35 million years ago during the late Eocene to Oligocene period of the Cenozoic Era. The mudstone of the Kobe Group is a geomaterial characterized by a high slaking rate and a low crushing rate. In the construction of the Sanyo Expressway between Kobe Junction and Miki-Ono Interchange, which is near this area, embankments were constructed without sufficient crushing and compaction of the embankment materials. The high slaking rate and low crushing rate of the embankment materials were a problem, after that, the slaking caused the embankment materials to become fine-grained, leading to large-scale compressive settlement in service (Shima and Imagawa, 1980). The "slaking rate" is a physical property determined by "NEXCO Test Method 110: Test method for slaking of rocks". This test is used to evaluate the durability of weak rocks. After measuring the mass of the sample in its natural state, it is oven dried at  $110 \pm 5^\circ\text{C}$  for 24 hours to measure the mass, and then it is immersed in water for 24 hours. After 5 cycles of dry and wet repetition of the same operation, the "slaking rate" is defined as the ratio of the dry mass passing the 9.5 mm sieve to the total dry mass. The greater the reduction, the lower the slaking resistance is evaluated. The "crushing rate" is a physical property value obtained by "NEXCO Test Method 109: Test method of crushing of rocks". In this test, rocks remaining on a 37.5mm to 19mm sieve are placed in a mold with an inner diameter of 150mm and loaded until the axial load reaches  $2\text{MN/m}^2$  to determine the degree of crushing.

(1) Chief, Geotechnics Division, Road Research Department, Nippon Expressway Research Institute Company Limited, Email: <t.abe.af@ri-nexco.co.jp>

(2) Researcher, Geotechnics Division, Road Research Department, Nippon Expressway Research Institute Company Limited, Email: <y.hashimoto.ab@ri-nexco.co.jp>

(3) Special senior researcher, Geotechnics Division, Road Research Department, Nippon Expressway Research Institute Company Limited

(4) DE, Professor, Graduate School of Engineering, Muroran Institute of Technology, Email: <skawamur@mmm.muroran-it.ac.jp>

Date of receipt: 15/4/2022  
Editing date: 6/5/2022  
Post approval date: 5/7/2022

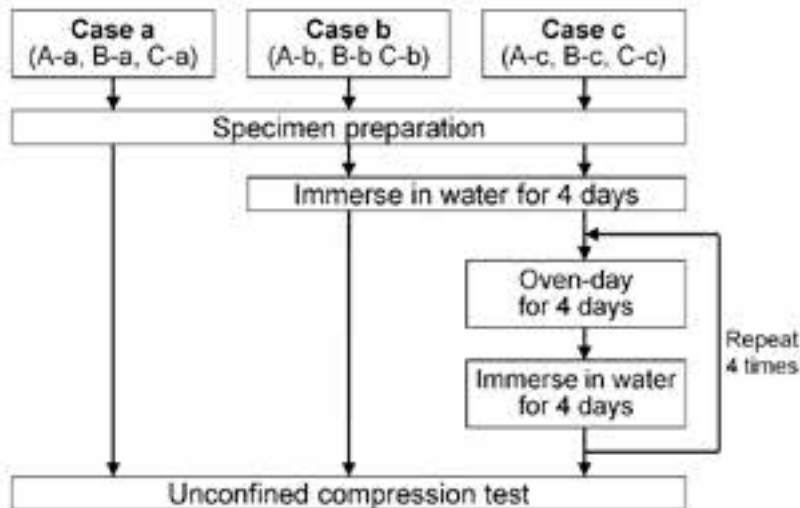


Figure 1: Flow chart of experiments

The ratio of the mass passing through the 9.5mm sieve after crushing to the total mass before loading is defined as the "crushing ratio. The higher the crushing ratio, the weaker the rock is.

Table 1: Physical properties of "Kobe 5" mudstone used in the experiments

Natural water content	$w_n$	17.4	%
Soil particle density	$\rho_s$	2.701	Mg/m <sup>3</sup>
Slaking rate		100	%
Crushing rate		44.0	%
Optimum water content	$w_{opt}$	22.5	%
Maximum grain size		300	mm

## 2.2. Experimental method

In the experiments, some of cylindrical specimens of 100mm in diameter and 200mm in height were prepared using this mudstone material (but with a maximum grain size of 37.5mm or less), and unconfined compression tests were conducted to determine those of unconfined compression strength. The conditions for preparing the specimens are shown in Table 2. Three different dry densities ( $\rho_d$ ) were set for the preparation of the specimens:  $\rho_{dA}$ ,  $\rho_{dB}$ , and  $\rho_{dC}$ . Thereafter, they are called the A series, B series, and C series, in each series. Three specimens under the same dry density were provided for each series. In preparing the specimens, the mudstone material was prepared so that the dry density ( $\rho_d$ ) was set for each series and the air content ( $v_a$ ) was 15%, and was statically compacted in four layers, one layer at a time, using an Amsler-type load testing machine. After that, unconfined compression tests were performed on three specimens, in each series, as shown in Figure 1. The unconfined compression test is specified in JIS A 1216 (2020) and applies compression to a cylindrical specimen continuously at a rate of 1% compressive strain per minute. During compression, a displacement meter measures the amount of compression  $\Delta H$  (mm) and a load cell measures the compressive force  $p$  (N). From the results, the compressive stress  $\sigma$  (kN/m<sup>2</sup>) and compressive strain  $\epsilon$  (%) are calculated and a stress-strain curve is drawn to determine the unconfined compressive strength  $q_u$  (kN/m<sup>2</sup>)

from the maximum compressive stress. One specimen was tested in its as-is condition (Case a) after specimen preparation, and the other one was tested after being immersed in water for four days (Case b). This Case b simulates the increase in water content in the embankment due to the infiltration of rainfall and groundwater into the embankment. The last other specimen was immersed in water for four days after specimen preparation, and then tested after five cycles of "four days of oven drying (110°C) and four days of water immersion" as one cycle (Case c). This Case c simulates how mudstone materials become finer due to the repeated action of drying and wetting after rainfall or groundwater infiltrates in the embankment.

Figure 2 illustrates the concept of these experiments. The compaction control standard for mudstone embankments (embankments using mudstone materials with a slaking rate of 30% or more and a crushing rate of 50% or less) on expressways managed by East Nippon Expressway Company, Central Nippon Expressway Company, and West Nippon Expressway Company (referred to as "NEXCO") requires that the dry density ( $\rho_d$ ) in the field be 90% or greater than the maximum dry density ( $\rho_{dmax}$ ) obtained by method B of "JIS A 1210 (2020): Test method for soil compaction using a rammer" and that the air content ( $v_a$ ) be 15% or less (the red hatch in Figure 2 (compaction curve) is applicable).

Table 2: Dry density and air content for each series of experiments

Series	Dry Density $\rho_d$ (Mg/m <sup>3</sup> )	Air Content $v_a$ (%)	Initial water content $w_0$ (%)
A	$\rho_{dA}$	15	$w_A (=w_n)$
B	$\rho_{dB} (\rho_{dmax} \times 0.93)$	15	$w_B$
C	$\rho_{dC} (\rho_{dmax} \times 0.90)$	15	$w_C$

The condition that satisfies this minimum compaction control standard is at point C-a ( $\rho_{dC} = \rho_{dmax} \times 0.9$ ,  $v_a = 15\%$ ) in Figure 2. In addition to point C-a, there are points A-a and B-a on the 15% air content curve. Point A-a is the dry density at natural water content ( $\rho_{dA} = \rho_{dwn}$ ), and Point B-a is the dry density between points A-a and C-a ( $\rho_{dB}$  was set to  $\rho_{dmax} \times 0.93$  for this test) to complement point A-a and point C-a. The condition of these specimens is the initial state (Case a) and is regarded as the condition immediately after the construction of the embankment. From these initial conditions, the process moves to the water absorption and retention process (Case b), which assumes rainfall and groundwater seepage, and the slaking process (Case c), which assumes fine graining of the mudstone materials by slaking.

The detailed explanation using the C series is as follows; Point C-a is the embankment that has been under the condition that satisfies the minimum compaction control standard. Subsequently, by immersing the specimen in water for four days, the dry density ( $\rho_{dC}$ ) does not change, but point C-a moves to point C-b as water seeps into the specimen and the water content increases (representing the

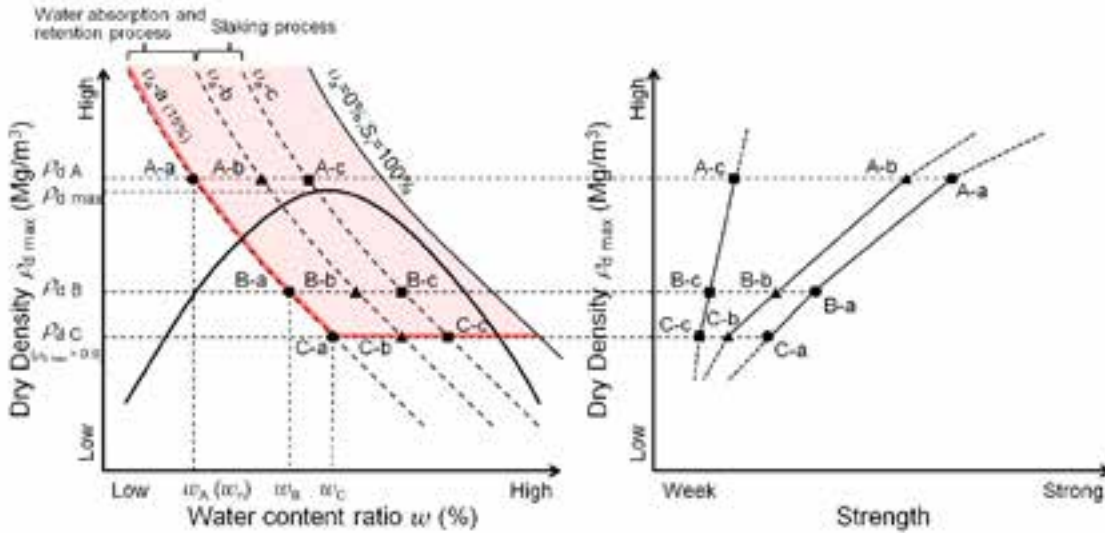


Figure 2: Conceptual diagram of experiments

water absorption and retention process of the embankment material). Furthermore, it is expected that the mudstone material in the specimen will become finer and water seepage will occur further in the specimen by repeating the drying and wetting process five times afterwards. At this time, the dry density does not change, but the water content increases, so the condition of the specimen changes from point C-b to point C-c, as shown in Figure 2 (representing the slaking process of the embankment material). By then determining the strength characteristics of each specimen, it would be possible to distinguish whether the reduction in strength of the mudstone embankment constructed was caused by the increase of water content due to rainwater and groundwater seepage, or whether the reduction in strength due to slaking.

2.3. Experimental results

Figure 3 shows the results of the experiments. Figure 3 embodies the conceptual diagram of the experiment shown in Figure 2 based on the results of the experiments. This one is also explained using the C series (point C-a, point C-b and point C-c) as an example. When the condition of the specimen changes from point C-a to point C-b, which is

the water absorption and retention course, the unconfined compression strength of the specimen decreases by about 40%. Furthermore, when the condition of the specimen changed from point C-b to point C-c, which assumes a fine-grained course due to slaking, the unconfined compression strength of the specimen was further decreased by about 30%. Similar trends were seen in the A series and B series.

3. Conclusions

The test results indicated that the reduction in strength of embankments constructed from slaking materials (referred to as "weak rock embankments") depends not only on the finer grain size of the embankment materials but also on the increase in water content. When slaking materials such as mudstone are excavated from the ground, they are on the dry side of the optimum water content. It is expected that the water content of weak rock embankments will naturally increase after the embankment is constructed due to water absorption and retention by rainwater and groundwater seepage. Since it is not easy to completely block the seepage of rainwater and groundwater, which are the sources of water supply, and a decrease in the strength of the weak rock embankments

(xem tiếp trang 62)

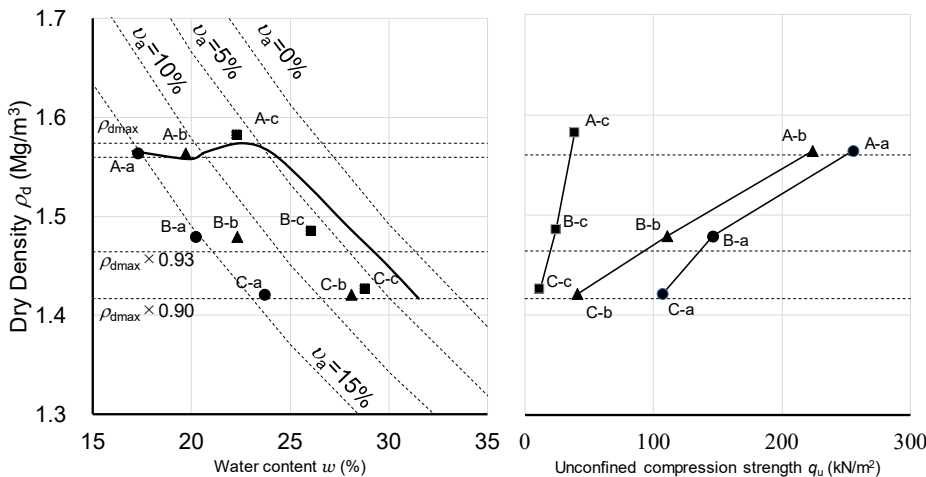


Figure 3: Relationship among dry density and water content and unconfined strength for each series

the CNN model demonstrated a high precision in detecting concrete cracks. In future studies, the proposed CNN application is recommended to integrate with a computer

and a camera system mounted on a vehicle to test the crack recognition capability of the software for the concrete road in Vietnam./

### References

1. Jong-Woo, K.; Sung-Bae, K.; Jeong-Cheon, P.; Jin-Won, N. Development of Crack Detection System with Unmanned Aerial Vehicles and Digital Image Processing. *Proceedings of the World Congress on Advances in Structural Engineering and Mechanics (ASEM15)*, Incheon, Korea, 25–29 August 2015; pp. 1–11.
2. Aldea, E.; Hégarat-Masclé, S.L. Robust crack detection for unmanned aerial vehicles inspection in a contrary decision framework. *J. Electr. Imaging* 2015, 24, 1–16, doi: 10.1117/1.JEI.24.6.061119.
3. Jinhong Chen, Haoting Liu, Jingchen Zheng, Ming Lv, Beibei Yan, Xin Hu, Yun Gao, Damage Degree Evaluation of Earthquake Area Using UAV Aerial Image. *International Journal of Aerospace Engineering*, Vol. 2016, Article ID 2052603, 10 pages, 2016. <https://doi.org/10.1155/2016/2052603>.
4. Peng, X., Zhong, X., Zhao, C., Chen, Y. F., Zhang, T. (2020). The Feasibility Assessment Study of Bridge Crack Width Recognition in Images Based on Special Inspection UAV. *Advances in Civil Engineering*, 2020, 8811649. <https://doi.org/10.1155/2020/8811649>.
5. S. Li and X. Zhao. Image-based concrete crack detection using convolutional neural network and exhaustive search technique. *Advances in Civil Engineering*, Vol. 2019.
6. Zhou, S., & Song, W. (2021). Deep learning-based roadway crack classification with heterogeneous image data fusion. *Structural Health Monitoring*, 20(3), 1274–1293. <https://doi.org/10.1177/1475921720948434>.
7. K. Simonyan and A. Zisserman. Very deep convolutional networks for large-scale image recognition. 2014, <https://arxiv.org/abs/1409.1556>.
8. C. Szegedy. Going deeper with convolutions. *Proceedings of the IEEE Conference on Computer Vision and Pattern Recognition*, pp. 1–9, Boston, MA, USA, June 2015.
9. K. He, X. Zhang, S. Ren, and J. Sun. Deep residual learning for image recognition. *Proceedings of the IEEE Conference on Computer Vision and Pattern Recognition*, pp. 770–778, Boston, MA, USA, June 2016.
10. L. Zhang, F. Yang, Y. D. Zhang, and Y. J. Zhu. Road crack detection using deep convolutional neural network. *Proceedings of the IEEE International Conference on Image Processing (ICIP)*, pp. 3708–3712, IEEE, Phoenix, AZ, USA, September 2016.
11. H. Maeda, Y. Sekimoto, T. Seto, T. Kashiyama, and H. Omata. Road damage detection using deep neural networks with images captured through a smartphone. 2018, <https://arxiv.org/abs/1801.09454>.
12. Z. Tong, J. Gao, and H. Zhang. Recognition, location, measurement, and 3D reconstruction of concealed cracks using convolutional neural networks. *Construction and Building Materials*, Vol. 146, pp. 775–787, 2017.
13. Nguyen, T. T., Ngoc, L. T., Vu, H. H., & Thanh, T. P. (2021). Machine learning-based model for predicting concrete compressive strength. *International Journal of Geomate*, 20(77), 197–204.
14. Nguyen, T.T., Pham, D. H., Pham, T.T., and Vu, H.H. (2020). Compressive strength evaluation of Fiber-Reinforced High Strength Self-Compacting Concrete with artificial intelligence. *Advances in Civil Engineering*, 2020, 3012139. <https://doi.org/10.1155/2020/3012139>.
15. Pham, T. T., Nguyen, T. T., Nguyen, L. N., Nguyen, P. V. (2020). A neural network approach for predicting hardened property of Geopolymer concrete. *International Journal of GEOMATE*, Oct. 2020, Vol.19, Issue 74, pp.193–201. ISSN: 2186-2982 (P), 2186-2990 (O), Japan, <https://doi.org/10.21660/2020.74.72565>.
16. Cha YJ, Choi W and Buyukozturk O. Deep learning-based crack damage detection using convolutional neural networks. *Comput Aided Civ Inf* 2017, 32: 361–378.
17. Dung CV. Autonomous concrete crack detection using deep fully convolutional neural network. *Automat Constr* 2019, 99: 52–58.
18. Srivastava N, Hinton G, Krizhevsky A. Dropout: a simple way to prevent neural networks from overfitting. *J Mach Learn Res* 2014, 15: 1929–1958.

## Strength reduction of mudstone embankment...

(tiếp theo trang 30)

due to increased water content is inevitable. For the reason, it is important to develop design and quality control methods for weak rock embankments that take into account the

reduction in strength due to water absorption and retention in order to improve durability and long-term performance./

### References

1. M. Takagi, S. Yokota, K. Suga, S. Yasuda and H. Ota. The actual situation of the slope of earthfill that collapsed by an earthquake disaster in the Tomei Expressway Makinohara district. 55th Geotechnical Engineering Symposium, 193–196, 2010 (in Japanese).
2. H. Nakamura. Study on Design and Construction Method of High Performance Embankment on Expressway. Doctoral Dissertation. Department of Environmental Field Engineering, Graduate School of Engineering, Hokkaido University, 2014 (in Japanese).
3. H. Shima and S. Imagawa. Compressive settlement of slaking materials (weak rock) and its countermeasures. *Tsuchi-to-Kiso*. Japan Geotechnical Society, Vol.28, No.7, 45–52, 1980 (in Japanese).
4. NEXCO Test Methods, Test method for slaking of rocks, NEXCO Test Method 110, 2015 (in Japanese).
5. NEXCO Test Methods, Test method of crushing of rocks, NEXCO Test Method 109, 2015 (in Japanese).
6. Japanese Industrial Standards, Method for unconfined compression test of soils, JIS A 1216, 2020.
7. Japanese Industrial Standards, Test method for soil compaction using a rammer, JIS A 1210, 2020.